Escola de Primavera de Transição e Turbulência
Blumenau 2022

ABCM
13th Spring School on Transition and Turbulence
September 19th-23rd, 2022, Blumenau, SC, Brazil

EPTT-2022-0013
INVESTIGATION OF TRANSITIONAL REGIME FLOW IN THE NETMIX MILLI-PHOTOREACTOR

Tatiana Matiazzo
Laboratory of Materials and Scientific Computing (LabMAC), Chemical and Food Engineering Department, Federal University of Santa Catarina, Campus Universitário Reitor João David Ferreira Lima, 88040-900, Florianópolis, Santa Catarina, Brazil.
tatiana.matiazzo@gmail.com

Vitor J. P. Vilar
Laboratory of Separation and Reaction Engineering – Laboratory of Catalysis and Materials (LSRE-LCM), Chemical Engineering Department, Faculty of Engineering, University of Porto, Rua Dr. Roberto Frias, 4200-465 Porto, Portugal.
vilar@fe.up.pt

Natan Padoin
Cíntia Soares
Laboratory of Materials and Scientific Computing (LabMAC), Chemical and Food Engineering Department, Federal University of Santa Catarina, Campus Universitário Reitor João David Ferreira Lima, 88040-900, Florianópolis, Santa Catarina, Brazil.
natan.padoin@ufsc.br
cintia.soares@ufsc.br

Abstract. *Continuous flow microfluids technology has several applications, including photocatalysis. The main challenges of photocatalytic reactors are related to photon and mass transfer. The velocity field inside a micro/milli-reactor influences the mass transfer. An important issue in microfluidics is related to slow mixing due to laminar flow in low Reynolds numbers. One alternative to improve mixing efficiency is to force the flow to be turbulent, which translates into fast diffusion, chaotic and continuous flow, great dissipation rate, multiscale eddies and 3D motion. There is still discussion into the possibility of such flow to be reached in milli/microfluidic devices due to its characteristic low Reynolds number. However, recent studies have shown the existence of turbulence in microchannels operating at a Reynolds number as low as 1. In the current work, the flow inside a milli-photocatalytic reactor known as NETmix was investigated for Reynolds numbers ranging from 0.2 to approximately 3,500. The pressure drop and the friction factor were evaluated in order to identify laminar and transitional flow regimes. A critical Reynolds number can be identified, indicating a clear laminar regime flow that presents a friction factor approximately equivalent to 32/Re and the region where transitional fluid flow begins.*

Keywords: *NETmix, Heterogeneous Photocatalysis, Turbulence, Microfluidics, Laminar Flow.*

1. INTRODUCTION

Static mixers are versatile devices that present high heat and mass transfer coefficients and for that have good applications for mixing and as reactors. This class of reactor is of particular interest for process intensification where the size of the equipment can be greatly reduce and the process efficiency increased (Meng *et al.*, 2020). Milli- and microfluidics are one of the possible approaches for process intensification (Shallan and Priest, 2019). Such devices have a wide range of chemical and biological applications and are characterized by a small size scale that do not surpass a few millimeters (Ward and Fan, 2015).

The pressure drop is considered an important variable for the selection and operation of static mixers. The pressure drop is often related to the friction factor (Michael *et al.*, 2022). Therefore, in this study the pressure drop and the friction factor are analyzed for the NETmix milli-reactor operating with water and air flow under Reynolds numbers between 0.2 and 3,500.

2. METHODOLOGY

2.1 NETmix Reactor and Static Mixer

The NETmix is a milli-reactor composed of a network of channels and chambers in a millimeter scale. The NETmix has been employed as a photocatalytic reactor and for that is composed of a stainless steel slab, where the pattern of circular chambers interconnected by prismatic channels is engraved, and a high transparency borosilicate glass slab that seals the reaction chamber. Fig. (1) depicts the NETmix reactor employed in this study. The characteristic dimensions of the employed NETmix are summarized in Tab. (1).

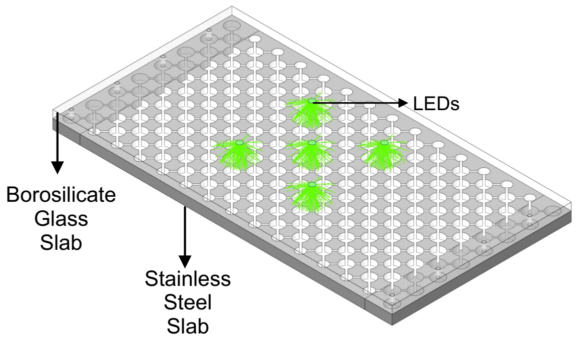

(a) NETmix system.

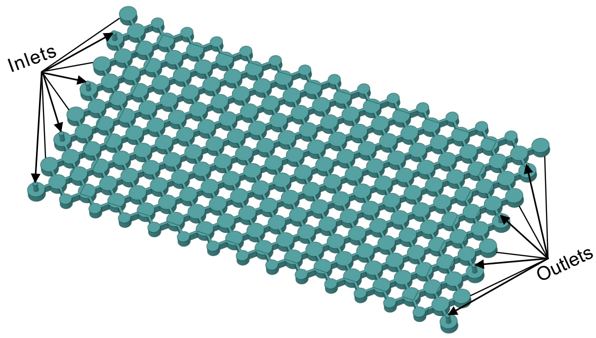

(b) Simulated geometry.

Figure 1: NETmix milli-reactor.

Table 1: Geometrical parameters.

NETmix Photoreactor	
Borosilicate glass slab thickness (mm)	4.0
Geometry depht (mm)	3.0
Window:	
Length (mm)	136.0
Width (mm)	76.0
Chambers:	
Diameter (mm)	6.5
Channels:	
Length (mm)	2.0
Width (mm)	1.0

2.2 CFD modeling and Simulated Cases

The flow of either water or air inside the NETmix was investigated here under isothermal steady state conditions considering incompressible Newtonian fluid with constant variables. The conservation of mass, momentum and species (Eqs. (1)-(7)) were solved in Ansys Fluent employing the realizable $k-\varepsilon$ model to account for turbulence in the system.

$$\nabla \cdot (\rho \boldsymbol{\nu}) = 0 \tag{1}$$

$$\nabla \cdot (\rho \boldsymbol{\nu}\boldsymbol{\nu} + \rho \boldsymbol{\nu}'\boldsymbol{\nu}') = -\nabla P - \nabla \cdot \boldsymbol{\tau} \tag{2}$$

$$\nabla \cdot (\rho \boldsymbol{\nu}\boldsymbol{\nu}) = -\nabla \mathbf{P} - \nabla \cdot \boldsymbol{\tau}^{\boldsymbol{eff}} \tag{3}$$

$$\boldsymbol{\tau}^{\boldsymbol{eff}} = \boldsymbol{\tau} + \boldsymbol{\tau_t} \tag{4}$$

$$\boldsymbol{\tau} = \mu \left(\nabla \boldsymbol{\nu} + \nabla \boldsymbol{\nu}^T\right) - \frac{2}{3}\mu \nabla \cdot \boldsymbol{\nu} I \tag{5}$$

$$\boldsymbol{\tau_t} = \rho \boldsymbol{\nu}'\boldsymbol{\nu}' \tag{6}$$

$$\nabla \cdot (\rho \boldsymbol{\nu} \boldsymbol{x_i} + \rho \boldsymbol{\nu}' \boldsymbol{x_i'}) = -\nabla \boldsymbol{J_i} \tag{7}$$

In total 44 simulations were performed, 22 simulations of air flowing inside the NETmix and 22 considering water flow. For both situations the temperature of the fluid was set as 298 K. The NETmix walls were set as no slip boundary condition. For the reactor inlet the velocity was prescribed as depicted in Tab. (2). At the reactor outlet, the gauge pressure was set as zero. The convergence criteria of the steady-state simulations was set as 10^{-4} for the momentum and continuity, 10^{-5} for species and 10^{-6} for energy. The structured mesh employed consists of a total of 10,785,298 hexahedron elements. Simulations were performed in a 64-bit Windows Server 2019 Datacenter equipped with Intel Xeon Gold 6126 CPU operating at 2.6 GHz, with access to 50 GB RAM memory. The CFD simulations were performed with 4 parallel solver processes.

Table 2: Simulated Conditions.

Case	Inlet Velocity (m/s)	$Re_{channels}$	Case	Inlet Velocity (m/s)	$Re_{channels}$
Case 1-Air	0.002	0.2	Case 1-Water	0.0003	0.2
Case 2-Air	0.004	0.4	Case 2-Water	0.0005	0.4
Case 3-Air	0.006	0.5	Case 3-Water	0.0008	0.6
Case 4-Air	0.008	0.8	Case 4-Water	0.001	0.7
Case 5-Air	0.01	1.0	Case 5-Water	0.0013	1.0
Case 6-Air	0.02	2.0	Case 6-Water	0.003	2.2
Case 7-Air	0.04	4.1	Case 7-Water	0.005	3.7
Case 8-Air	0.06	5.1	Case 8-Water	0.008	5.9
Case 9-Air	0.08	7.6	Case 9-Water	0.01	7.4
Case 10-Air	0.1	10.1	Case 10-Water	0.013	9.6
Case 11-Air	0.2	20.1	Case 11-Water	0.03	22.0
Case 12-Air	0.4	39.8	Case 12-Water	0.05	36.4
Case 13-Air	0.6	54.5	Case 13-Water	0.08	57.8
Case 14-Air	0.8	73.8	Case 14-Water	0.1	71.9
Case 15-Air	1.0	93.0	Case 15-Water	0.13	93.0
Case 16-Air	2.0	182.9	Case 16-Water	0.3	210.0
Case 17-Air	4.0	357.9	Case 17-Water	0.5	344.9
Case 18-Air	6.0	531.2	Case 18-Water	0.8	545.7
Case 19-Air	8.0	691.1	Case 19-Water	1.0	675.0
Case 20-Air	10.0	874.2	Case 20-Water	1.3	869.0
Case 21-Air	20.0	1,727.9	Case 21-Water	3.0	1,976.0
Case 22-Air	40.0	3,454.5	Case 22-Water	5.0	3,276.1

3. RESULTS AND DISCUSSIONS

To evaluate the pressure drop and the friction factor simulations for the flow of air and water were carried out for a variety of Reynolds numbers in the NETmix milli-reactor. Figure (2) depicts how the pressure drop increases in the NETmix reactor with the augment of Reynolds number.

The Reynolds number inside the channels of the reactor was varied from 0.2 to around 3,500 in numerical simulations. The pressure drop registered for an air stream varied from 0.05 Pa to approximately 35,000 Pa. For a water stream the pressure drop ranged from 0.2 Pa to about 122,000 Pa.

For laminar flows, the dependency of ΔP with the Reynolds number is linear due to the Hagen-Poiseuille equation, but in the presence of vortex structures this dependency becomes a square law (Khaydarov *et al.*, 2018). In the NETmix case, for Reynolds numbers lower than 10 this linear dependency was verified and the pressure drop can be expressed as $\Delta P = 0.3Re$ for the air flow and $\Delta P = 1.1Re$ for water flow. Covering a wider range of Reynolds numbers a square law

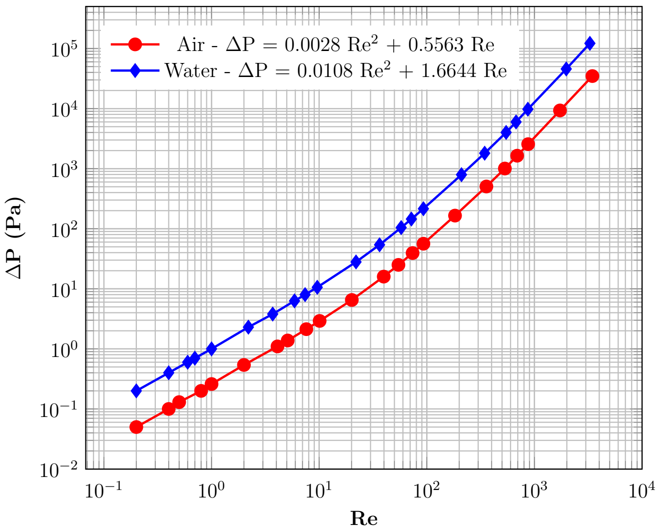

Figure 2: Pressure drop for distinct Reynolds numbers.

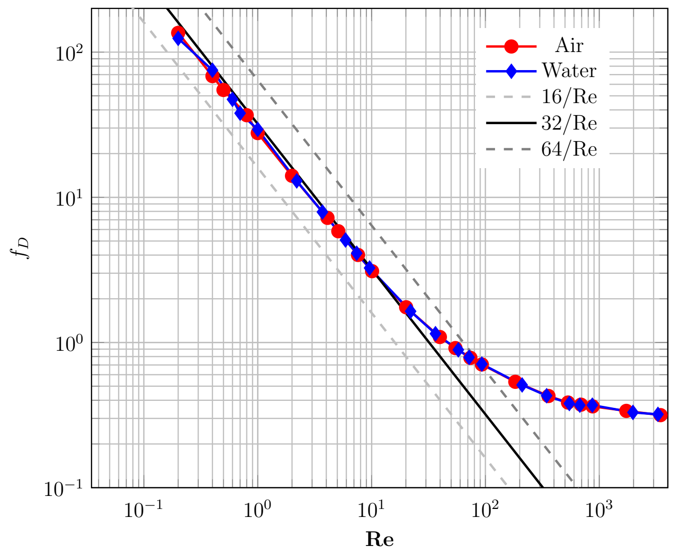

Figure 3: Friction factor calculated at distinct Reynolds numbers.

can describe the pressure drop in the reactor as ΔP = 0.0028Re^2+0.5663Re and ΔP = 0.0108Re^2+1.6644Re for air and water, respectively.

The Darcy friction factor (Eq. (8)) normalizes the pressure drop based on inertial scales and it is a dimensionless form to evaluate the flow resistance (Nguyen *et al.*, 2021). For Reynolds numbers above 10 the friction factor increases potentially with the increase of Reynolds number and tends to reach and stabilize at a value of around 0.5.

$$f_D = \frac{2}{\nu^2}\frac{d_h}{l}\frac{\Delta P}{\rho} \tag{8}$$

where ΔP (Pa) is the pressure drop, l (m) is the length of the reactor, ρ (kg/m^3) is the density of the fluid, v (m/s) is the velocity and d_h (m) is the hydraulic diameter.

In Fig. (3) the friction factor calculated at each Reynolds number is displayed for both air and water flows. For comparison an f_D = 32/Re is plotted alongside the results. For low Reynolds numbers the friction factor was approximately equivalent to 32/Re.

Therefore, the analysis of the pressure drop and the friction factor suggests that for the NETmix milli-reactor the laminar-to-transition region is located at a low Reynolds number. For Reynolds numbers above only 10 transitional behavior can be found. These analysis is reinforced by the observation of velocity streamlines inside the NETmix. Figure (4) depicts the velocity streamlines found for selected cases.

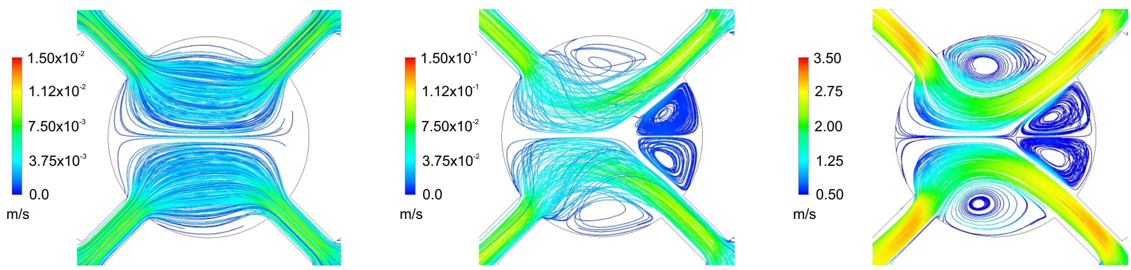

(a) Case 10-water, Re$_{channels}$ = 9.6. (b) Case 15-water, Re$_{channels}$ = 93. (c) Case 22-water, Re$_{channels}$ = 3,276.

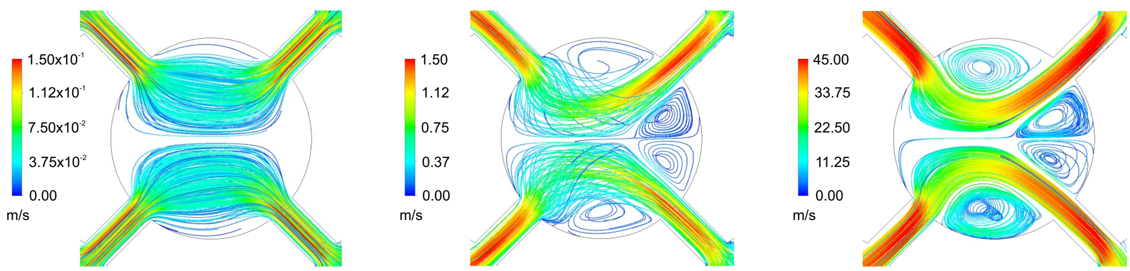

(d) Case 10-air, Re$_{channels}$ = 10.1. (e) Case 15-air, Re$_{channels}$ = 93. (f) Case 22-air, Re$_{channels}$ = 3,455.

Figure 4: Velocity streamlines in the NETmix milli-reactor.

In Fig. (4a) and Fig. (4d) the streamlines of water and air flow, respectively, are depicted for a Reynolds number of about 10. The figures demonstrates the ordered laminar like flow registered in this conditions. For Reynolds numbers close to 100 (Fig. (4b) for water flow and Fig. (4e) for air flow) and Reynolds numbers above 3,000 (Fig. (4c) for water flow and Fig. (4f) for air flow) the streamlines illustrate the presence of several recirculation patterns inside the NETmix chambers that induce transitional and turbulent like behavior at low Reynolds numbers.

4. CONCLUSIONS

In the current work, the laminar to transition regime flow in a milli-reactor known as NETmix was investigated for both liquid and gaseous flow. A total of 44 CFD simulations were carried out to evaluate the flow of either air or water.

The pressure drop and the friction factor were employed to inquire the laminar to transition flow behavior. Flows with Reynolds numbers ranging from 0.2 to almost 3,500 were analyzed. Under these conditions the pressure drop ranged from 0.05 Pa to about 35,000 Pa in the case of air flow and between 0.2 to around 122,000 Pa for water flow.

It was found that the behavior of both pressure drop and friction factor has been altered for Reynolds numbers as low as 10. For Reynolds numbers under 10, the flow behaves as laminar, with pressure drop having linear dependency with Reynolds number and presenting a friction factor equivalent to 32/Re. Increasing the Reynolds number above 10, removes the linear dependency of pressure drop with Re and the flow inside the circular chambers of the NETmix milli-reactor show several recirculations patterns compatible with transitional and turbulence behavior.

5. ACKNOWLEDGEMENTS

The authors acknowledge Ansys Inc. and ESSS for the support and software license lease. The authors acknowledge CAPES (Coordination for the Improvement of Higher-Level Personnel), CAPES-PRINT Project Number 88887.310560/2018-00, and CNPq (National Council for Scientific and Technological Development), process number 141088/2018-4, for the financial support. This work was also financially supported by: Base-UIDB/50020/2020 and Programmatic-UIDP/50020/2020 Funding of LSRE-LCM, funded by national funds through FCT/MCTES (PIDDAC). Vítor J.P. Vilar acknowledges the FCT Individual Call to Scientific Employment Stimulus 2017 (CEECIND/01317/2017).

6. REFERENCES

Khaydarov, V., Borovinskaya, E.S. and Reschetilowski, W., 2018. "Numerical and experimental investigations of a micromixer with chicane mixing geometry". *Applied Sciences*, Vol. 8, No. 12.

Meng, H., Han, M., Yu, Y., Wang, Z. and Wu, J., 2020. "Numerical evaluations on the characteristics of turbulent flow and heat transfer in the lightnin static mixer". *International Journal of Heat and Mass Transfer*, Vol. 156, p. 119788.

Michael, V., Dawson, M., Prosser, R. and Kowalski, A., 2022. "Laminar flow and pressure drop of complex fluids in a sulzer smx+tm static mixer". *Chemical Engineering Research and Design*, Vol. 182, pp. 157–171.

Nguyen, Q.M., Abouezzi, J. and Ristroph, L., 2021. "Early turbulence and pulsatile flows enhance diodicity of Tesla's macrofluidic valve". *Nature Communications*, Vol. 12, No. 1, p. 2884.

Shallan, A.I. and Priest, C., 2019. "Microfluidic process intensification for synthesis and formulation in the pharmaceutical industry". *Chemical Engineering and Processing - Process Intensification*, Vol. 142, p. 107559.

Ward, K. and Fan, Z.H., 2015. "Mixing in microfluidic devices and enhancement methods". *J. Micromech. Microeng.*, Vol. 25, No. 9, p. 094001.

7. RESPONSIBILITY NOTICE

The authors are the only responsible for the printed material included in this paper.